EUROPEAN ORGANIZATION FOR NUCLEAR RESEARCH

Coherent J/ψ photoproduction at midrapidity in Pb–Pb collisions at $\sqrt{s_{\mathrm{NN}}} = 5.02$ TeV

ALICE Collaboration*

Abstract

The coherent J/ψ photoproduction cross section is measured for the first time at midrapidity in peripheral to semicentral Pb–Pb collisions at $\sqrt{s_{\mathrm{NN}}} = 5.02$ TeV. The centrality differential cross section $\mathrm{d}\sigma/\mathrm{d}y$ is reported for the centrality range 40–90%, together with the doubly-differential cross section $\mathrm{d}^2\sigma/\mathrm{d}y\mathrm{d}p_{\mathrm{T}}$, extracted in two peripheral centrality classes. The J/ψ mesons are reconstructed in the dielectron channel, in the rapidity interval $|y| < 0.9$ using the ALICE central barrel detectors. The J/ψ cross section at midrapidity is statistically compatible to the earlier ALICE measurement at forward rapidity and at the same centre-of-mass energy, and shows only a mild centrality dependence over the covered range. Several sets of theoretical calculations taking into account the hadronic overlap in the collisions but ignoring possible final-state effects from a hot expanding medium are found to give a fairly good description of the current measurements within uncertainties.

---

*See Appendix A for the list of collaboration members

1 Introduction

In ultrarelativistic collisions between heavy ions, the Lorentz-contracted nuclei generate strong electromagnetic fields, and either of them can be treated as the source of a quasi-real photon, which interacts with the other nucleus treated as the target. The photoproduction cross section can be factorised as the product of the photon flux emanating from one of the colliding nuclei, which is proportional to the square of the nuclear electric charge, Z^2, and the photonuclear cross section. This process can be viewed as a fluctuation of the photon into a quark-antiquark pair (colour dipole), which then interacts with the gluon field of the target nucleus, at leading order through the exchange of two gluons in a colour singlet state, producing a real vector meson [1]. In this approximation, the cross section is proportional to the square of the target gluon distribution at relevant values of (x, Q^2) [2]. The photoproduction can be either coherent, with the photon interacting with the target nucleus as a whole, generating a vector meson with very low transverse momentum ($\langle p_T \rangle \sim 60$ MeV/c), or incoherent, with the photon interacting with a single nucleon, producing a meson of higher transverse momentum ($\langle p_T \rangle \sim 500$ MeV/c) [3]. Photonuclear vector meson production is thus a powerful tool for investigating the gluonic structure of the target. Cross section measurements are sensitive to the gluon density in the nucleus and, due to the relatively low values of x that are accessible via this process, may constitute a probe for gluon shadowing or saturation. In addition, spatial characteristics of the gluon distribution, such as transverse size, shape, and fluctuations, can be accessed through measurements of the differential cross section $d\sigma/dt$, with the Mandelstam variable $t \sim -p_T^2$ [4].

Photonuclear reactions have been most extensively studied in ultraperipheral collisions (UPC) of heavy ions, taking place at impact parameters larger than the sum of their radii. With combinatorial and hadronic backgrounds being negligible, coherent and incoherent cross sections can readily be extracted. At the LHC energies, ALICE, CMS and LHCb have studied coherent charmonium photoproduction in ultraperipheral Pb–Pb collisions at $\sqrt{s_{NN}} = 2.76$ TeV [5–7] and 5.02 TeV [4, 8–12], in the rapidity ranges $|y| < 0.9$ (ALICE), $1.8 < |y| < 2.3$ (CMS, 2.76 TeV), $1.6 < |y| < 2.4$ (CMS, 5.02 TeV), $2.5 < y < 4$ (ALICE) and $2.0 < y < 4.5$ (LHCb).

Coherent photoproduction of J/ψ in heavy-ion interactions with nuclear overlap, manifesting as a prominent excess (for $p_T < 0.3$ GeV/c) relative to the soft tail of the hadronically generated J/ψ spectrum, was first observed by ALICE in peripheral Pb–Pb collisions at $\sqrt{s_{NN}} = 2.76$ TeV and at forward rapidity ($2.5 < y < 4$), in the centrality range 30–90% [13]. The phenomenon was confirmed by STAR at RHIC energies, in Au–Au (20–80%) and U–U (40–80%) collisions at $\sqrt{s_{NN}} = 200$ and 193 GeV, respectively, also presenting the p_T and $|t|$ dependence of the coherent cross section [14]. Recently, LHCb [15] and ALICE [16] reported a similar excess also in Pb–Pb collisions at $\sqrt{s_{NN}} = 5.02$ TeV, in both cases measured at forward rapidity ($2 < y < 4.5$ and $2.5 < y < 4$, respectively). LHCb, covering a range of peripheral collisions (approximately 65–90%), measured the differential J/ψ photoproduction yield dN/dy as a function of the number of participants $\langle N_{part} \rangle$ and y, and the doubly-differential yield d^2N/dydp_T as a function of p_T. ALICE extracted the coherent J/ψ photoproduction centrality differential cross section dσ/dy over the centrality range 0–90%, setting an upper limit for the most central collisions (0–10%). A mild centrality dependence is revealed, compatible within uncertainties both with a flat trend and with a decrease of the cross section towards more central collisions.

The observation of coherent photoproduction in nuclear collisions with overlap inspired new theoretical developments [17–23], attempting to quantitatively describe the centrality, rapidity, and in the case of Refs. [19, 20, 23], the p_T dependence of the experimentally measured cross sections or yields. In order to account for the hadronic overlap, these models take the UPC picture as a baseline and impose geometric constraints implemented as impact parameter ranges, modifying the photon flux and, in some cases, also the photonuclear cross section.

Several questions remain unresolved regarding coherent photoproduction processes in a hadronic envi-

ronment, including the roles of spectator and participant nucleons as photon sources and targets (theoretically explored in [19]), the survival of the coherence condition in the presence of nuclear breakup, and the time ordering of the hadro- and photoproduction. The coherent J/ψ p_T distribution, its impact parameter dependence, and the possible influence of destructive interference between the two photon sources and of the strong interactions in the nuclear overlap zone have been investigated in Refs. [19, 20]. The shapes of the measured $|t|$ spectrum in Ref. [14] and p_T spectrum in Ref. [15] are well reproduced by these calculations within uncertainties. However, no available experimental data allow meaningful assessment of the evolution of p_T distributions with collision centrality.

An issue still sparsely explored by models is the potential influence of the hot and rapidly expanding partonic medium generated in the hadronic overlap zone on the coherently photoproduced, low-p_T charmonia. The latter are formed during the same narrow time interval as the initial hadronic interactions occur, presumably distributed over the surface of the target nuclei [22], and remain almost stationary in the transverse plane. This subset of the observable J/ψ population is uniquely identifiable as primordial survivors through their characteristic p_T distribution, and is, therefore, a particularly interesting QGP probe. Possible final-state medium effects are expected to be nearly absent in the most peripheral collisions, but may exhibit an onset with increasing nuclear overlap, manifesting as a reduction in measured cross sections and possibly a modulation in azimuthal distributions beyond that predicted by models considering only geometric constraints on photoproduction. Taking into account gluon-induced dissociation of charmonia in the plasma, Ref. [22] predicts a medium-induced suppression of the photoproduced J/ψ yield of $\sim$ 20–40% for semicentral collisions with $\langle N_{part} \rangle \sim$ 100–150.

This paper presents for the first time the J/ψ coherent photoproduction cross section, measured at midrapidity in peripheral to semicentral (40–90%) Pb–Pb collisions at $\sqrt{s_{NN}}$ = 5.02 TeV. The doubly-differential cross section $d^2N/dydp_T$ extracted by ALICE is reported for the first time for J/ψ photoproduction in collisions with nuclear overlap for two centrality classes, 50–70% and 70–90%. Section 2 gives an overview of the experimental apparatus and the data sample used, while Section 3 details the analysis and the extraction of systematic uncertainties. Section 4 presents the results and discusses them in the context of other existing J/ψ photoproduction measurements and relevant model calculations. Finally, Section 5 summarises the conclusions based on the LHC Run 2 data and points to opportunities offered by upcoming high-luminosity runs.

2 Experimental setup and data sample

A detailed description of the ALICE detector and its performance is provided in Refs. [24, 25]. In this work, J/ψ mesons are reconstructed in the dielectron channel at midrapidity ($|y| < 0.9$), using the central barrel charged particle tracking detectors ITS (Inner Tracking System) [26] and TPC (Time Projection Chamber) [27] which provide very good tracking and electron identification in the pseudorapidity range $|\eta| < 0.9$. The ITS comprises six cylindrical detection layers based on different silicon technologies, surrounding the beam axis at radii ranging from 3.9 to 43 cm. The two innermost layers, requiring the highest granularity, are Silicon Pixel Detectors (SPD), while the two middle layers are Silicon Drift Detectors (SDD) and the two outermost ones are Silicon Strip Detectors (SSD). The ITS system is used for the determination of the event primary interaction point, precision tracking for the location of secondary vertices from weakly decaying particles, and event selection. The TPC is a cylindrical gaseous detector, filled with a mixture of argon and carbon dioxide, surrounding the ITS, with an inner radius of 0.85 m, an outer radius of 2.5 m, and a length of 5 m along the beam direction. It is the main tracking detector of the central barrel system, also performing particle identification based on the specific energy loss dE/dx in the gas.

In addition, a suite of detectors for global event characterisation is employed. The V0 detector [28] consists of two scintillating arrays covering the pseudorapidity ranges $2.8 < \eta < 5.1$ (V0A) and $-3.7 < \eta < -1.7$

(V0C), both being segmented in pseudorapidity and azimuthal angle. This subsystem is used for trigger-ing and rejecting beam-induced background events, measuring charged particle multiplicity, and deter-mining collision centrality and event plane azimuthal angle. The centrality in Pb–Pb collisions is defined as the percentile of the hadronic cross section corresponding to the charged particle multiplicity mea-sured in the V0 detector [29]. A fit of a Glauber Monte Carlo model to the V0 amplitude distribution is used to relate the experimental centrality with geometric quantities like the average impact parameter ($\langle b \rangle$) and the number of participants ($\langle N_{\text{part}} \rangle$). The Zero Degree Calorimeter [30] comprises two sets of detector arrays located close to the beam axis on both sides of the nominal interaction point, at a distance of $\pm$ 112.5 m. Their task is detecting nucleons emitted at zero degrees relative to the beam axis, aiding event characterisation both in hadronic and electromagnetic interactions, and rejection of beam-induced background.

The analysed data set was collected by ALICE during the 2015 and 2018 LHC Pb–Pb runs at $\sqrt{s_{\text{NN}}} = 5.02$ TeV. At midrapidity, data was acquired using the minimum bias (MB) trigger, defined by the coincidence of signals in both the V0A and V0C arrays. In the 2018 period, a central and a semicentral trigger were used in addition. These were defined using the MB trigger in combination with thresholds on the total online signal amplitude in the V0 detector, corresponding roughly to collision centralities of 0–10% and 30–50%, respectively. In this analysis, only events from the centrality range 40–90% were considered. Beam-induced background was rejected using timing information from the V0 and the Zero Degree Calorimeter detectors. All events were required to have a reconstructed primary vertex with a longitudi-nal position within ± 10 cm from the nominal interaction point. Events with pileup occurring during the TPC readout time were rejected in the offline analysis based on the correlation between the number of TPC and ITS (SDD+SSD) clusters. After all selections, the number of analysed events is approximately 37 million, 35 million, and 35 million for the 40–50%, 50–70%, and 70–90% centrality ranges, respec-tively. This corresponds to an integrated luminosity of $\sim 49.6~\mu\text{b}^{-1}$ for the 40–50% centrality interval and $\sim 24~\mu\text{b}^{-1}$ for both the 50–70% and 70–90% centrality intervals [31].

3   Data analysis

The J/ψ mesons are reconstructed using the e^+e^- decay channel. The selected electron candidates are good quality tracks reconstructed through both the ITS and TPC, with a minimum total momentum (p) of 1 GeV/c and a pseudorapidity $|\eta| < 0.9$. To ensure excellent tracking quality, each track is required to have a minimum number of 70 associated space points in the TPC and a maximum calculated χ^2/N_{dof} value of 2 for the fit of the track to the clusters. Secondary particles are suppressed by requiring the maximum distance-of-closest-approach (DCA) of the track to the interaction vertex to be 1 cm in the transverse and 3 cm in the longitudinal direction. In addition, daughters of long-lived weakly decaying particles are removed using topological selections. In order to improve the tracking resolution and to reduce the number of secondary electrons from photon conversions in the detector material, at least one hit in either of the two SPD layers is required. Electrons and positrons are identified via their specific energy loss in the TPC gas by selecting a band of width $\pm 3\sigma_e$ around the electron expectation value estimated from a parameterisation of the measured average dE/dx as a function of momentum [32], with σ_e being the resolution of this measurement. To further reduce the contamination from hadrons, tracks with a dE/dx compatible with the pion or proton hypothesis within $\pm 3.5\sigma_{\pi/p}$, are rejected. Finally, electrons from photon conversions are further suppressed by using a prefiltering method [33] where candidate tracks forming a pair with invariant mass $m_{ee} < 50$ MeV/c^2 when combined with a set of candidates selected using looser cuts, are excluded from the analysis.

In order to extract the yields of coherently photoproduced J/ψ, a two-dimensional distribution $N(m_{ee}, p_{\text{T}})$ is constructed from all combinations of opposite-sign electron tracks from the same event and passing all selections described above. An unbinned 2-dimensional log-likelihood fitting procedure is applied to the measured distribution using a model which includes contributions from photoproduction ($F_{\text{phot,i}}$),

hadroproduction (F_{hadr}), and background (F_{bkg}):

$$F(m_{ee}, p_T) = f_{bkg} \cdot F_{bkg}(m_{ee}, p_T) + f_{hadr} \cdot F_{hadr}(m_{ee}, p_T) + f_{phot} \cdot \sum_i w_{phot,i} F_{phot,i}(m_{ee}, p_T) , \qquad (1)$$

where f_{bkg}, f_{hadr}, and f_{phot} are the normalisation parameters of the respective components, and $w_{phot,i}$ are the fractional contributions from the different photoproduction processes, all described in more detail below.

The background component, F_{bkg}, is constructed as the sum of the combinatorial background and a much smaller background contribution from correlated semileptonic decays of heavy-quark pairs. The combinatorial background, F_{bkg}^{comb}, is constructed using the mixed-event technique, pairing opposite-sign electrons from events with similar global characteristics (centrality, vertex position, and event plane orientation). It is normalised using the like-sign pairs according to the expression

$$F_{bkg}^{comb}(m_{ee}, p_T) = N^{ME-OS}(m_{ee}, p_T) \cdot \frac{\sum_{m_{ee}^i, p_T^j} N^{SE-LS}(m_{ee}^i, p_T^j)}{\sum_{m_{ee}^i, p_T^j} N^{ME-LS}(m_{ee}^i, p_T^j)}, \qquad (2)$$

where N^{ME-OS} is the distribution of opposite-sign mixed-event pairs, while N^{SE-LS} and N^{ME-LS} are the like-sign pair distributions from the same and mixed events, respectively, summed over the m_{ee} and p_T. More details on the mixed-event procedure can be found in Refs. [34]. The two-dimensional correlated background component, F_{bkg}^{corr}, is constructed using a parameterisation of the residual background obtained from the (m_{ee}, p_T) dielectron distribution by subtracting the combinatorial background. The parameterisation is a 2D function which is factorisable into a first-order polynomial over the invariant mass dimension and a piecewise polynomial function over the p_T dimension. The correlated background component has a relatively small amplitude compared to the combinatorial background and to the J/ψ signal as well as to statistical fluctuations. The unbinned likelihood fit is therefore performed both with and without this component, yielding a small difference taken as a systematic uncertainty, as described later in this section. Due to the fact that F_{bkg}^{comb} is already normalised via Eq. 2, F_{bkg}^{corr} and the total sum F_{bkg} will also be normalised by construction, and the corresponding parameter f_{bkg} is therefore fixed in the fit of Eq. 1.

The two-dimensional hadroproduction component, F_{hadr}, is estimated via a Monte-Carlo simulation, described in more detail in Refs. [35, 36]. This MC used a realistic kinematic distribution of inclusive unpolarised J/ψ based on existing measurements, including a fit to inclusive yields reported in Ref. [35]. The J/ψ were embedded in an underlying environment of Pb–Pb collisions generated using HIJING 1.0 [37]. The p_T shape of the embedded J/ψ signal was further tuned to match the p_T differential J/ψ yields recently measured by ALICE in the relevant centrality classes [36]. The J/ψ decay is forced into the dielectron channel using the PHOTOS package [38]. The simulated particles were transported through a model of the ALICE detector using GEANT3 [39], and then reconstructed with the same algorithms as used for real data.

The photoproduction component, $\Sigma_i w_{phot,i} F_{phot,i}$, is a sum of contributions from several processes, i, namely: coherent and incoherent J/ψ photoproduction, feed-down from coherently and incoherently photoproduced $\psi(2S)$, incoherent J/ψ photoproduction with nucleon dissociation, and continuum $\gamma\gamma \to e^+e^-$. The processes were simulated using the STARLight generator [40] with the same relative weights as those obtained in the UPC analysis reported in Ref. [9], and embedded into Pb–Pb collisions generated using the HIJING model with a similar setup as the one described for the hadronic component. Integrated in the range $p_T < 0.2$ GeV/c, the ratio between the incoherent, feed-down and $\gamma\gamma$ continuum to the coherent J/ψ component is approximately 1%, 2.5% and 11%, respectively. The charmonia generated with STARLight are transversely polarised, as expected from s-channel helicity conservation and recently confirmed experimentally for coherently photoproduced J/ψ [41]. For the incoherent J/ψ with nucleon
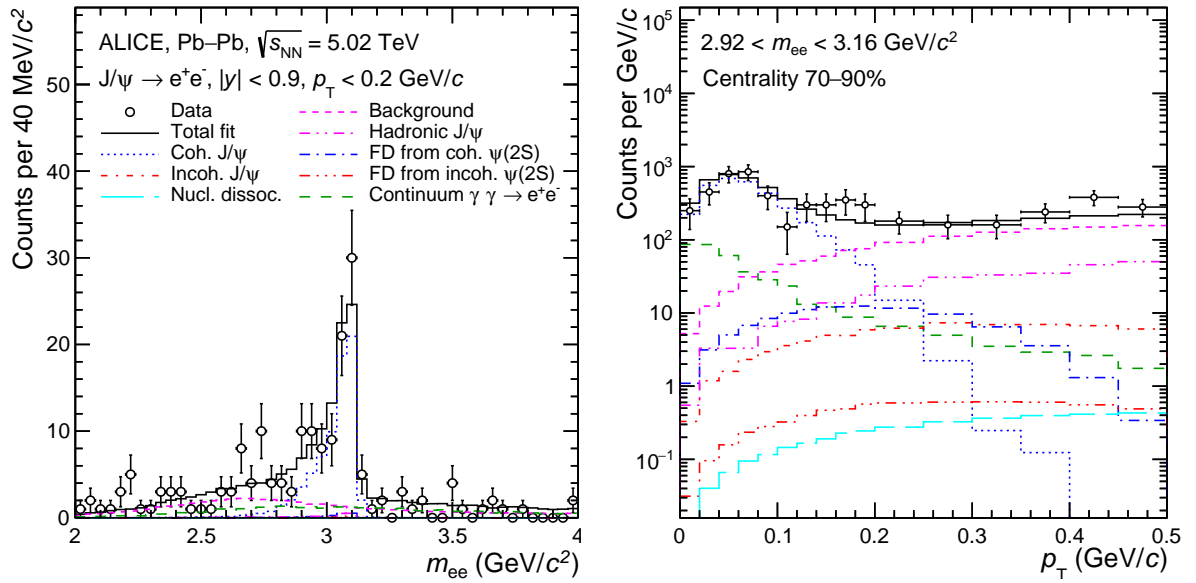
Figure 1: Invariant mass distribution for $p_T < 200$ MeV/c (left panel) and p_T distribution for $2.92 < m_{ee} < 3.16$ GeV/c^2 (right panel) in the centrality class 70–90% for dielectrons with $|y| < 0.9$ in Pb–Pb collisions at $\sqrt{s_{NN}} = 5.02$ TeV. Measured distributions for J/ψ candidates are shown as black markers and the fit components as coloured lines, as explained in the legend.

dissociation component, a process not incorporated in STARLight, the p_T shape was constructed using the H1 parameterisation [42]. The individual two-dimensional template shapes of the various processes, $F_{\mathrm{phot},i}(m_{ee}, p_T)$, were obtained from the reconstructed electron pairs using the same reconstruction algorithm and analysis selections as for the data. The sum of all the reconstructed and weighted templates is used as a single component in the unbinned fit of Eq. 1 due to the fact that the size of the current data set does not allow the normalisation factors ($f_{\mathrm{phot}} \cdot w_{\mathrm{phot},i}$) of all these templates to vary independently in the fit.

In order to extract the signal, the unbinned data $N(m_{ee}, p_T)$ is fitted with the model from Eq. 1, where the only free parameters are f_{hadr} and f_{phot}. The fit is performed in the p_T range $0 < p_T < 7$ GeV/c and the mass range $2 < m_{ee} < 4$ GeV/c^2. This procedure is performed in the centrality classes 40–50%, 50–70%, and 70–90%, and the raw yield of coherently photoproduced J/ψ, $N_{\mathrm{J}/\psi,\mathrm{coh}}$, is found by integrating the corresponding fitted template function for $p_T < 0.2$ GeV/c and $2.92 < m_{e^+e^-} < 3.16$ GeV/c^2. The quality of the fitting procedure is illustrated in Fig. 1. The left panel shows a projection on the invariant mass dimension for candidate pairs with $p_T < 0.2$ GeV/c for Pb–Pb collisions in the 70–90% centrality range. The right panel shows a projection on the p_T dimension for pairs in the invariant mass interval $2.92 < m_{e^+e^-} < 3.16$ GeV/c^2 and the same centrality range. The two projections of the candidate pair distribution are compared to the projection from the fit model and its various components as described above.

The doubly-differential cross section of the coherent J/ψ photoproduction, $\mathrm{d}^2\sigma/\mathrm{d}y\mathrm{d}p_T$, for a rapidity interval, Δy, and a p_T interval, Δp_T, is computed as:

$$\frac{\mathrm{d}^2\sigma}{\mathrm{d}y\mathrm{d}p_T} = \frac{N_{\mathrm{J}/\psi,\mathrm{coh}}}{(A \times \varepsilon)_{\mathrm{J}/\psi,\mathrm{coh}} \times BR(\mathrm{J}/\psi \to \mathrm{e^+e^-}) \times \Delta y \times \Delta p_T \times \mathscr{L}} , \qquad (3)$$

where $N_{\mathrm{J}/\psi,\mathrm{coh}}$ is the raw yield of coherently photoproduced J/ψ, $(A \times \varepsilon)_{\mathrm{J}/\psi,\mathrm{coh}}$ is the average acceptance and efficiency factor for the kinematic window studied, and $\mathscr{L}$ is the integrated luminosity for the analysed data sample as given in Sec. 2, all referring to the centrality class considered. The obtained

computed cross sections correspond to the luminosity integrated in the given centrality interval. The $BR(\mathrm{J}/\psi \to \mathrm{e^+e^-})$ is the branching ratio of the J/ψ decay into the dielectron channel [43].

The acceptance times efficiency correction is the product of the kinematic acceptance, the tracking and particle identification (PID) efficiency, and the fraction of the signal contained within the invariant mass counting window. With the exception of the PID efficiency, all these factors are obtained based on a MC simulation of coherently photoproduced, transversely polarised J/ψ generated using STARLight and embedded in Pb–Pb collisions generated using HIJING, as described above. The J/ψ PID efficiency is estimated using a data-driven method, similar to the one described in Ref. [34, 36], based on a pure sample of electrons using tagged photon conversions. The total acceptance times efficiency correction is about 10% on average, with a p_T dependence which for the contributing factors listed above is quite mild in the $p_\mathrm{T} < 0.5$ GeV/c range relevant here. However, there is some p_T migration between generator and detector level due to the J/ψ p_T resolution being of the same order as the typical p_T of the coherent photoproduced J/ψ, and due to the radiative J/ψ decay. The impact of bin migration was checked by applying an unfolding procedure to the measured raw spectrum, as described later in this section, and the differences were found to be negligible.

The systematic uncertainties affecting the measured cross sections originate from uncertainties on the tracking and particle identification efficiencies, signal extraction, collision centrality, luminosity determination, and the branching ratio of the J/ψ into dielectrons. A summary of all the uncertainties is provided in Table 1. The tracking uncertainty consists of two contributions, one from the ITS-TPC matching and one due to the choice of the track quality criteria, as also detailed in Ref. [34]. The former is taken as the difference observed between MC simulations and data for the single-track ITS-TPC matching efficiency, propagated to J/ψ candidate dielectrons, and amounts to about 6.5%. The latter is estimated by repeating the analysis with variations of the track quality criteria and amounts to approximately 3.3%. The uncertainty on the PID efficiency is estimated by varying the pion and proton exclusion cuts, as described in Refs. [34, 36], and resulted in an uncertainty of 2.1% for the 40–50% and 3.8% for the 50–90% centrality ranges. The uncertainty on the signal extraction includes contributions from the templates used in the fit model described in Eq. 1, fit ranges, and signal counting method. The F_bkg template was changed by removing the correlated background component and thus keeping only the combinatorial component estimated with event mixing. Adopting a rather conservative approach, the F_hadr component is constructed with and without the tuning of the input p_T shape on experimental data, and the associated systematic error is taken as $1/\sqrt{12}$ of the difference of the resulting cross sections, corresponding to the ratio of the standard deviation and the full spread of a uniform distribution. The corresponding uncertainties from the F_bkg and F_hadr variations range between 0.2–4.1% and 0.6–1.1%, respectively. The F_phot template corresponding to the coherent photoproduction process was varied from its shape expected for UPC, assuming that the $\langle p_\mathrm{T} \rangle$ of the distribution is inversely proportional to the radius of the target nucleus spectator region, with the radius being determined for each centrality range as $R \sim A_\mathrm{spec}^{1/3}$, with $A_\mathrm{spec} = A_\mathrm{Pb} - \langle N_\mathrm{part} \rangle / 2$. Hence, the template shapes were modified for each centrality interval by shifting each entry in the original STARLight-generated template from p_T to rp_T, with $r = (A_\mathrm{Pb}/A_\mathrm{spec})^{1/3}$, plus a Gaussian smearing term, centred at zero, to avoid binning effects. The J/ψ yields extracted with these modified templates deviated from the default between 0.15 and 3.1%, depending on centrality, with the deviation growing towards more central collisions as expected. Variations of the fit ranges in invariant mass and transverse momentum led to systematic uncertainties between 0.35 and 2.2%, depending on centrality. The default signal counting method, integrating the J/ψ coherent photoproduction template, was changed to counting the entries left after subtracting all the other fit components. The extracted yields changed by 18.5%, 3.5%, and 1.3% for the centrality ranges 40–50%, 50–70%, and 70–90%, respectively. The uncertainty on the integrated luminosity is 2.5% and is determined in the analysis of the van der Meer scan runs as described in Ref. [44]. The uncertainty on the centrality selection is determined by running the analysis with centrality ranges shifted by 1% in either direction to account for uncertainties on the anchor point used in the centrality definition [45]. The varia-

tions of the extracted yields are compatible with statistical fluctuations, but we conservatively assigned a systematic uncertainty of 1% for the most peripheral centrality range and 2% for the rest. For the (y, p_T) doubly-differential cross sections, the systematic uncertainties are considered to a large extent correlated over p_T and uniform (global) in the p_T range relevant for coherent J/ψ photoproduction. An exception is the uncertainty due to the fit procedure, which is also strongly correlated over p_T; however, the size of the uncertainties have point-to-point variations and thus are not considered as global. The uncertainty on the J/$\psi \to e^+e^-$ branching ratio is quoted as 0.5% [43].

Two methodical cross checks were performed for the analysis. For the first one, the fixed weights $w_{phot,i}$ adopted from Ref. [9] for the photoproduced components $F_{phot,i}$, were grouped according to their origin: the weights for the coherent and incoherent charmonium production plus the $\gamma\gamma \to e^+e^-$ continuum were left free in the fit, while keeping the same ratio as in Ref. [9] between feed-down and direct production for the coherent and incoherent components. This approach gave very similar results to the default method, and no associated systematic error was assigned. The second cross check involved using an unfolding procedure instead of the acceptance times efficiency correction to obtain the doubly-differential cross sections, in order to quantify possible effects due to the J/ψ kinematic variation between the generator and detector level. The response matrix was constructed using the MC simulations for coherently photoproduced J/ψ, and the unfolding was performed using both the Bayes [46] and Single Value Decomposition [47] methods with different values for the regularisation parameter. The difference relative to the default method was found to be negligible in this case as well, and no systematic uncertainty was assigned.

Table 1: Systematic uncertainties on the coherent J/ψ cross section for different centrality intervals. The systematic sources marked with a ($*$) are considered to be correlated over centrality. All the systematic uncertainty sources are considered fully correlated over p_T.

Centrality	40–50%	50–70%	70–90%
Tracking (cut variations)*	3.3%	3.3%	3.3%
Tracking (ITS-TPC matching)*	6.5%	6.5%	6.5%
Electron identification*	2.1%	3.8%	3.8%
Fit (correlated bkg)	4.1%	0.4%	0.2%
Fit (hadronic J/ψ)	0.6%	1.3%	1.1%
Fit (coherent J/ψ)	3.1%	0.7%	0.15%
Fit range	2.2%	1.0%	0.4%
Signal extraction method	18.5%	3.5%	1.3%
Luminosity*	2.5%	2.5%	2.5%
Centrality definition*	2%	2%	1%
Branching ratio*	0.5%	0.5%	0.5%
Total	21.1%	9.7%	8.9%

4 Results

The left panel of Fig. 2 shows the coherent J/ψ photoproduction cross section dσ/dy, extracted at midrapidity ($|y| < 0.9$), as a function of $\langle N_{part} \rangle$, for the centrality classes 70–90%, 50–70%, and 40–50%. Systematic uncertainties (excluding the global contribution from the beam luminosity) are depicted as open boxes, while the global centrality-independent systematic uncertainty of 2.5% is quoted in the legend. The measured cross sections show a mild centrality dependence, within uncertainties compatible with no variation within the studied centrality range. It should be noted that, as pointed out in the Sec. 3, the cross sections are integrated in their respective centrality intervals and that the three data points cover different fractions of the total Pb–Pb cross section. Namely, the semicentral data point (40–50%)
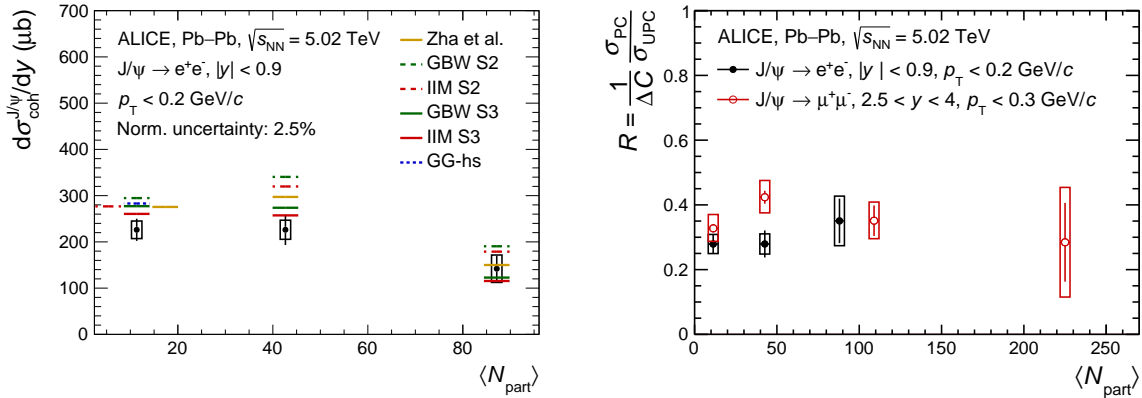
Figure 2: Left: Coherent J/ψ cross section as a function of $\langle N_{\mathrm{part}} \rangle$ in Pb–Pb collisions at $\sqrt{s_{\mathrm{NN}}}$ = 5.02 TeV at midrapidity. The statistical uncertainties are shown as bars, while the systematic uncertainties (excluding the global contribution from the beam luminosity) are shown as boxes. It should be noted that the interval 40–50% is half as wide as the two more peripheral ones, 50–70%, and 70–90%. Data are compared to calculations from W. Zha *et al.* [19, 20], Gay-Ducati *et al.* (GBW S2/S3 and IIM S2/S3) [17] and Cepila *et al.* (GG-hs) [18]. For the interval 70–90%, the calculations from W. Zha *et al.* and IIM S2 are shifted on the x-axis for visibility. Right: Coherent J/ψ cross section as a function of $\langle N_{\mathrm{part}} \rangle$ measured at midrapidity (black markers) and forward rapidity (red markers) [16] normalised to the corresponding cross sections measured in the same rapidity ranges in UPC [8, 9] and corrected for the centrality interval width ΔC.

covers 10% while the two most peripheral data points each cover 20% of the total cross section. The experimental results are compared with a set of theoretical models, as indicated in the legend.

The calculations are based on the UPC description of vector meson photoproduction in terms of a convolution of the photon flux and the photonuclear cross section, but integrating only over the impact parameter range corresponding to the centrality class of interest. The overlapping region in the collision, with hadronic interactions, is considered in some of the calculations by introducing modifications of the photon flux and/or the photonuclear cross section, depending on the model. The GG-hs model by Cepila *et al.* [18] includes no modifications relative to the UPC picture except the specification of the impact parameter interval. Attempting to describe both coherent and incoherent photoproduction, this model employs an energy-dependent representation of subnucleonic degrees of freedom. This is modelled in terms of hot spots and a colour-dipole proton cross section taking low-x saturation effects into account [48], and using the Glauber-Gribov formalism to extrapolate the calculation from nucleonic to nuclear targets. In the set of predictions by Gay-Ducati *et al.* [17] labelled GBW and IIM, an effective photon flux is defined by integrating over photons reaching the nuclear target and disregarding those hitting the overlap region. These calculations consider two scenarios, denoted in Fig. 2 as S2 and S3, with S2 modifying the photon flux only while S3 in addition restricts the photonuclear cross section, excluding contributions from the hadronically interacting overlap zone. The GBW [48] and the IIM [49] descriptions employ different treatments of saturation effects in the colour-dipole proton cross section, based on parameterisations of DIS data. The approach by Zha *et al.* [19, 20] takes into account the potential effect on photon and gluon emission by the hadronically interacting overlapping zone, exploring different scenarios regarding the roles of participants and spectators. In addition, these calculations consider the implications of the destructive interference between the photon amplitudes from the two nuclear sources moving in opposite directions. The estimates from Ref. [20] shown in Fig. 2 include nuclear shadowing effects and assume an unaltered photon emission from the overlapping region except for interference effects, combined with the disruption of photoproduction in the participant region.

The experimental results are qualitatively well described by the model calculations, although for the two
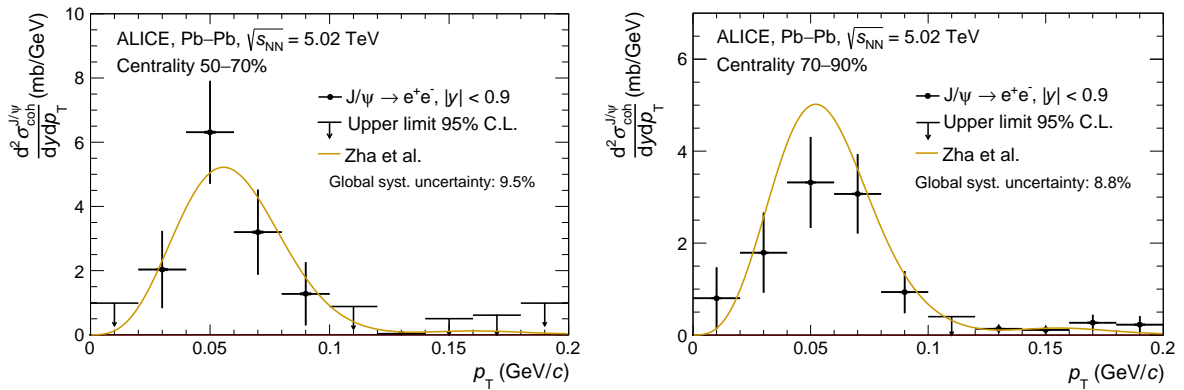
Figure 3: Coherent J/ψ cross section as a function of p_T in Pb–Pb collisions at $\sqrt{s_{NN}} = 5.02$ TeV measured in the 50–70% and 70–90% centrality classes. The error bars indicate statistical uncertainties, while the systematic uncertainties, excluding those considered as global (see text for details), are shown as boxes. Data are compared to calculations from W. Zha *et al.* [19, 20].

most peripheral intervals, the absolute values of the cross sections are overestimated by all models. In particular, the calculations by Gay-Ducati *et al.* [17] for scenario S3, which take into account suppression of photoproduction in the overlap zone, are the most compatible with the data with a statistical significance of the differences averaged over the three centrality intervals of less than 2σ. However, the S2 scenario from Ref. [17] overestimates the measured cross section for all studied centrality intervals and the statistical compatibility with the data is around 3σ. It is worth noting that a modification of the photonuclear cross section might not be the only mechanism that explains the data. ALICE measurements at forward rapidity [16], which are qualitatively similar in trend and model comparisons to the results at midrapidity, are well described by the calculations by Klusek-Gawenda [21], which only assume inhibition of the photon flux in the overlap region.

The comparison with data at forward rapidity might also provide information on any final-state QGP influence on photoproduced charmonia. Such effects are naively expected to be more pronounced at midrapidity, where a higher medium temperature and energy density is expected [50]. The J/ψ photoproduction at mid- and forward rapidity are compared after normalising the measurements to the coherent J/ψ photoproduction cross section measured in UPC in the same rapidity interval in order to compensate for the rapidity dependence. Uncertainties which are correlated between the results in collisions with overlap and those in UPC are cancelled in the ratio. There are also two small differences in the kinematic coverage of the UPC results compared to those from peripheral or semicentral collisions. Namely, the midrapidity UPC coherent J/ψ yield is measured at $|y| < 0.8$ and the p_T range for the forward-rapidity one is $p_T < 0.25$ GeV/c. This ratio (σ_{PC}/σ_{UPC}), corrected for the different centrality interval widths ΔC, is shown in the right panel of Fig. 2 as a function of $\langle N_{part} \rangle$, for forward ($2.5 < y < 4$) and midrapidity ($|y| < 0.9$). The measurements at forward rapidity in peripheral collisions are taken from Ref. [16], while the UPC results for the two rapidity intervals are from Refs. [8, 9]. Within uncertainties, the ratios at the two rapidities are statistically compatible over the common centrality range, and show a nearly flat evolution with $\langle N_{part} \rangle$. Notably, the measurements for the most peripheral collisions, 70–90%, which are also the most precise, are in very good agreement. The measured cross sections in this analysis show no hints of QGP effects, but the centrality range studied is rather limited, extending only up to $\langle N_{part} \rangle < 100$, which, combined with the large experimental uncertainties, may be insufficient to reveal any medium-induced suppression. The large increase in luminosity to be collected during the LHC Run 3 and 4 is expected to extend the range of the J/ψ measurement up to the most central collisions and also give access to the centrality dependent photoproduction of the less bound ψ(2S), important for shedding light on these phenomenological aspects.

10

Figure 3 shows the doubly-differential cross section $\mathrm{d}^2\sigma/\mathrm{d}y\mathrm{d}p_\mathrm{T}$ for the rapidity interval $|y| < 0.9$ and in the centrality classes 50–70% (left) and 70–90% (right), which was obtained by subtracting from the measured distribution $N(m_\mathrm{ee}, p_\mathrm{T})$ all of the fitted templates with the exception of the one corresponding to the coherently photoproduced J/ψ. The p_T-independent systematic uncertainties are quoted in the legend for the two centralities as global uncertainties, while the point-to-point systematic uncertainties related to the fit of the two-dimensional $(m_\mathrm{ee}, p_\mathrm{T})$ pair distributions are shown as boxes around the data points and are very small compared to the global ones and the statistical uncertainties. The theoretical calculations by Zha *et al.*, described above [19, 20], in which the nucleons in the overlapping zone do not participate in the photoproduction, are in good agreement with ALICE measurements within the large experimental uncertainties. This model was also found to reproduce the shape of the LHCb p_T differential measurements, but appears to underpredict the reported yield [15]. In the model, the rapid decline of the cross section towards $p_\mathrm{T} = 0$ is ascribed to the destructive interference between photon amplitudes from the two collision partners, while the bulk of the distribution and the tail towards higher p_T carry information about the target size and spatial distribution. In particular, a variation of the p_T differential cross section is expected with centrality. The observed shapes of the p_T spectra in the 50–70% and 70–90% centrality classes are compatible with the current experimental uncertainties, however, only a very weak centrality dependence is predicted in this centrality range, as seen from the theory calculation shown in Fig. 3.

5 Conclusions

In summary, this paper reports on the measurement of coherent J/ψ photoproduction cross section as a function of p_T and collision centrality, for peripheral and semicentral Pb–Pb collisions at $\sqrt{s_\mathrm{NN}} = 5.02$ TeV, for the first time at midrapidity ($|y| < 0.9$) at LHC energies. The reported observations extend and complement earlier measurements published by ALICE and LHCb at forward rapidity, and STAR at midrapidity at a lower collision energy. The p_T-integrated cross section exhibits a mild centrality dependence compatible with no variation over the centrality interval studied and is qualitatively similar to the corresponding observations at forward rapidity. Within the large uncertainties, the centrality-dependent measurements are fairly well described by several sets of theoretical calculations, based on the UPC description of vector meson photoproduction and modified to take into account the nuclear overlap in the collisions, but not incorporating effects from a hot expanding QGP. The combined ALICE measurements at mid- and forward rapidity favour models with inhibition of photon flux only, or inhibition of the photon flux together with a suppression of charmonium generation in the hadronic overlap region. Within uncertainties, the measured cross sections show no suppression beyond the present model predictions. The p_T-integrated cross sections measured at mid- and forward rapidity by ALICE, normalised to the cross sections measured in the same rapidity ranges in UPC [8, 9], are in good agreement within uncertainties. The p_T-differential cross sections are well described by calculations taking into account the interference between the two photon emitters as well as the effect of strong interactions in the overlap zone. Future data-taking campaigns during the LHC Run 3 and Run 4 [51], with a foreseen increase in statistics of a factor of about 100 at midrapidity, are expected to facilitate photoproduction measurements for central collisions (0–10%) and precision measurements of p_T-differential cross sections for non-central collisions (above 10%). This will help elucidate the influence of the nuclear overlap region on the coherent J/ψ photoproduction, including possible final-state effects from the expanding QGP.

References

[1] S. R. Klein and H. Mäntysaari, "Imaging the nucleus with high-energy photons", *Nature Rev. Phys.* **1** (2019) 662–674, `arXiv:1910.10858 [hep-ex]`.

[2] A. J. Baltz *et al.*, "The Physics of Ultraperipheral Collisions at the LHC", *Phys. Rept.* **458** (2008) 1–171, `arXiv:0706.3356 [nucl-ex]`.

[3] C. A. Bertulani, S. R. Klein, and J. Nystrand, "Physics of ultra-peripheral nuclear collisions", *Ann. Rev. Nucl. Part. Sci.* **55** (2005) 271–310, `arXiv:nucl-ex/0502005`.

[4] **ALICE** Collaboration, S. Acharya *et al.*, "First measurement of the $|t|$-dependence of coherent J/ψ photonuclear production", *Phys. Lett. B* **817** (2021) 136280, `arXiv:2101.04623 [nucl-ex]`.

[5] **ALICE** Collaboration, B. Abelev *et al.*, "Coherent J/ψ photoproduction in ultra-peripheral Pb-Pb collisions at $\sqrt{s_{NN}} = 2.76$ TeV", *Phys. Lett. B* **718** (2013) 1273–1283, `arXiv:1209.3715 [nucl-ex]`.

[6] **ALICE** Collaboration, E. Abbas *et al.*, "Charmonium and e^+e^- pair photoproduction at mid-rapidity in ultra-peripheral Pb-Pb collisions at $\sqrt{s_{NN}}$=2.76 TeV", *Eur. Phys. J. C* **73** (2013) 2617, `arXiv:1305.1467 [nucl-ex]`.

[7] **CMS** Collaboration, V. Khachatryan *et al.*, "Coherent J/ψ photoproduction in ultra-peripheral PbPb collisions at $\sqrt{s_{NN}} = 2.76$ TeV with the CMS experiment", *Phys. Lett. B* **772** (2017) 489–511, `arXiv:1605.06966 [nucl-ex]`.

[8] **ALICE** Collaboration, S. Acharya *et al.*, "Coherent J/ψ photoproduction at forward rapidity in ultra-peripheral Pb-Pb collisions at $\sqrt{s_{NN}} = 5.02$ TeV", *Phys. Lett. B* **798** (2019) 134926, `arXiv:1904.06272 [nucl-ex]`.

[9] **ALICE** Collaboration, S. Acharya *et al.*, "Coherent J/ψ and ψ' photoproduction at midrapidity in ultra-peripheral Pb-Pb collisions at $\sqrt{s_{NN}} = 5.02$ TeV", *Eur. Phys. J. C* **81** (2021) 712, `arXiv:2101.04577 [nucl-ex]`.

[10] **LHCb** Collaboration, R. Aaij *et al.*, "Study of coherent J/ψ production in lead-lead collisions at $\sqrt{s_{NN}} = 5$ TeV", *JHEP* **07** (2022) 117, `arXiv:2107.03223 [hep-ex]`.

[11] **ALICE** Collaboration, S. Acharya *et al.*, "Energy dependence of coherent photonuclear production of J/ψ mesons in ultra-peripheral Pb-Pb collisions at $\sqrt{s_{NN}} = 5.02$ TeV", *JHEP* **10** (2023) 119, `arXiv:2305.19060 [nucl-ex]`.

[12] **CMS** Collaboration, A. Tumasyan *et al.*, "Probing Small Bjorken-x Nuclear Gluonic Structure via Coherent J/ψ Photoproduction in Ultraperipheral Pb-Pb Collisions at $\sqrt{s_{NN}}$ =5.02 TeV", *Phys. Rev. Lett.* **131** (2023) 262301, `arXiv:2303.16984 [nucl-ex]`.

[13] **ALICE** Collaboration, J. Adam *et al.*, "Measurement of an excess in the yield of J/ψ at very low p_T in Pb-Pb collisions at $\sqrt{s_{NN}} = 2.76$ TeV", *Phys. Rev. Lett.* **116** (2016) 222301, `arXiv:1509.08802 [nucl-ex]`.

[14] **STAR** Collaboration, J. Adam *et al.*, "Observation of excess J/ψ yield at very low transverse momenta in Au+Au collisions at $\sqrt{s_{NN}} = 200$ GeV and U+U collisions at $\sqrt{s_{NN}} = 193$ GeV", *Phys. Rev. Lett.* **123** (2019) 132302, `arXiv:1904.11658 [hep-ex]`.

[15] **LHCb** Collaboration, R. Aaij *et al.*, "J/ψ photoproduction in Pb-Pb peripheral collisions at $\sqrt{s_{NN}}$= 5 TeV", *Phys. Rev. C* **105** (2022) L032201, `arXiv:2108.02681 [hep-ex]`.

[16] **ALICE** Collaboration, S. Acharya *et al.*, "Photoproduction of low-p_{T} J/ψ from peripheral to central Pb−Pb collisions at 5.02 TeV", *Phys. Lett. B* **846** (2023) 137467, `arXiv:2204.10684` `[nucl-ex]`.

[17] M. B. Gay Ducati and S. Martins, "Heavy meson photoproduction in peripheral AA collisions", *Phys. Rev. D* **97** (2018) 116013, `arXiv:1804.09836` `[hep-ph]`.

[18] J. Cepila, J. G. Contreras, and M. Krelina, "Coherent and incoherent J/ψ photonuclear production in an energy-dependent hot-spot model", *Phys. Rev. C* **97** (2018) 024901, `arXiv:1711.01855` `[hep-ph]`.

[19] W. Zha, S. R. Klein, R. Ma, L. Ruan, T. Todoroki, Z. Tang, Z. Xu, C. Yang, Q. Yang, and S. Yang, "Coherent J/ψ photoproduction in hadronic heavy-ion collisions", *Phys. Rev. C* **97** (2018) 044910, `arXiv:1705.01460` `[nucl-th]`.

[20] W. Zha, L. Ruan, Z. Tang, Z. Xu, and S. Yang, "Double-slit experiment at fermi scale: coherent photoproduction in heavy-ion collisions", *Phys. Rev. C* **99** (2019) 061901, `arXiv:1810.10694` `[hep-ph]`.

[21] M. Kłusek-Gawenda and A. Szczurek, "Photoproduction of J/ψ mesons in peripheral and semicentral heavy ion collisions", *Phys. Rev. C* **93** (2016) 044912, `arXiv:1509.03173` `[nucl-th]`.

[22] W. Shi, W. Zha, and B. Chen, "Charmonium Coherent Photoproduction and Hadroproduction with Effects of Quark Gluon Plasma", *Phys. Lett. B* **777** (2018) 399–405, `arXiv:1710.00332` `[nucl-th]`.

[23] L. Jenkovszky, V. Libov, and M. V. T. Machado, "Regge phenomenology and coherent photoproduction of J/ψ in peripheral heavy ion collisions", *Phys. Lett. B* **827** (2022) 137004, `arXiv:2202.02162` `[hep-ph]`.

[24] **ALICE** Collaboration, K. Aamodt *et al.*, "The ALICE experiment at the CERN LHC", *JINST* **3** (2008) S08002.

[25] **ALICE** Collaboration, B. B. Abelev *et al.*, "Performance of the ALICE Experiment at the CERN LHC", *Int. J. Mod. Phys. A* **29** (2014) 1430044, `arXiv:1402.4476` `[nucl-ex]`.

[26] **ALICE** Collaboration, K. Aamodt *et al.*, "Alignment of the ALICE Inner Tracking System with cosmic-ray tracks", *JINST* **5** (2010) P03003, `arXiv:1001.0502` `[physics.ins-det]`.

[27] J. Alme *et al.*, "The ALICE TPC, a large 3-dimensional tracking device with fast readout for ultra-high multiplicity events", *Nucl. Instrum. Meth.* **A622** (2010) 316–367, `arXiv:1001.1950` `[physics.ins-det]`.

[28] **ALICE** Collaboration, E. Abbas *et al.*, "Performance of the ALICE VZERO system", *JINST* **8** (2013) P10016, `arXiv:1306.3130` `[nucl-ex]`.

[29] **ALICE** Collaboration, B. Abelev *et al.*, "Centrality determination of Pb-Pb collisions at $\sqrt{s_{NN}} =$ 2.76 TeV with ALICE", *Phys. Rev. C* **88** (2013) 044909, `arXiv:1301.4361` `[nucl-ex]`.

[30] R. Arnaldi *et al.*, "The Zero degree calorimeters for the ALICE experiment", *Nucl. Instrum. Meth. A* **581** (2007) 397–401. [Erratum: Nucl.Instrum.Meth.A 604, 765 (2009)].

[31] **ALICE** Collaboration, S. Acharya *et al.*, "ALICE luminosity determination for Pb−Pb collisions at $\sqrt{s_{\text{NN}}} =$ **5.02** TeV",. `https://cds.cern.ch/record/2749127`.

[32] W. Blum, L. Rolandi, and W. Riegler, *Particle detection with drift chambers*. Particle Acceleration and Detection. Springer, 2008.

[33] **ALICE** Collaboration, S. Acharya *et al.*, "Inclusive J/ψ production at mid-rapidity in pp collisions at $\sqrt{s}$ = 5.02 TeV", *JHEP* **10** (2019) 084, arXiv:1905.07211 [nucl-ex].

[34] **ALICE** Collaboration, S. Acharya *et al.*, "Inclusive J/ψ production at midrapidity in pp collisions at $\sqrt{s} = 13$ TeV", *Eur. Phys. J. C* **81** (2021) 1121, arXiv:2108.01906 [nucl-ex].

[35] **ALICE** Collaboration, S. Acharya *et al.*, "Centrality and transverse momentum dependence of inclusive J/ψ production at midrapidity in Pb–Pb collisions at $\sqrt{s_{\mathrm{NN}}}$ =5.02 TeV", *Phys. Lett. B* **805** (2020) 135434, arXiv:1910.14404 [nucl-ex].

[36] **ALICE** Collaboration, S. Acharya *et al.*, "Measurements of inclusive J/ψ production at midrapidity and forward rapidity in Pb–Pb collisions at $\sqrt{s_{\mathrm{NN}}} = 5.02$ TeV", *Phys. Lett. B* **849** (2024) 138451, arXiv:2303.13361 [nucl-ex].

[37] X.-N. Wang and M. Gyulassy, "HIJING: A Monte Carlo model for multiple jet production in pp, pA, and AA collisions", *Phys. Rev. D* **44** (1991) 3501–3516.

[38] P. Golonka and Z. Was, "PHOTOS Monte Carlo: A Precision tool for QED corrections in *Z* and *W* decays", *Eur. Phys. J. C* **45** (2006) 97–107, arXiv:hep-ph/0506026.

[39] R. Brun, F. Bruyant, M. Maire, A. C. McPherson, and P. Zanarini, *GEANT 3: User's guide Geant 3.10, Geant 3.11; rev. version*. CERN, Geneva, 1987. https://cds.cern.ch/record/1119728.

[40] S. R. Klein, J. Nystrand, J. Seger, Y. Gorbunov, and J. Butterworth, "STARlight: A Monte Carlo simulation program for ultra-peripheral collisions of relativistic ions", *Comput. Phys. Commun.* **212** (2017) 258–268, arXiv:1607.03838 [hep-ph].

[41] **ALICE** Collaboration, S. Acharya *et al.*, "First polarisation measurement of coherently photoproduced J/ψ in ultra-peripheral Pb−Pb collisions at $\sqrt{s_{\mathrm{NN}}} = 5.02$ TeV", arXiv:2304.10928 [nucl-ex].

[42] **H1** Collaboration, C. Alexa *et al.*, "Elastic and Proton-Dissociative Photoproduction of J/ψ Mesons at HERA", *Eur. Phys. J. C* **73** (2013) 2466, arXiv:1304.5162 [hep-ex].

[43] **Particle Data Group** Collaboration, S. Navas *et al.*, "Review of particle physics", *Phys. Rev. D* **110** (2024) 030001.

[44] **ALICE** Collaboration, S. Acharya *et al.*, "ALICE luminosity determination for Pb−Pb collisions at $\sqrt{s_{\mathrm{NN}}} = 5.02$ TeV", *JINST* **19** (2024) P02039, arXiv:2204.10148 [nucl-ex].

[45] **ALICE** Collaboration, S. Acharya *et al.*, "Centrality determination in heavy ion collisions",. https://cds.cern.ch/record/2636623. ALICE-PUBLIC-2018-011.

[46] G. D'Agostini, "A Multidimensional unfolding method based on Bayes' theorem", *Nucl. Instrum. Meth. A* **362** (1995) 487–498.

[47] A. Hocker and V. Kartvelishvili, "SVD approach to data unfolding", *Nucl. Instrum. Meth. A* **372** (1996) 469–481, arXiv:hep-ph/9509307.

[48] K. J. Golec-Biernat and M. Wusthoff, "Saturation effects in deep inelastic scattering at low Q^2 and its implications on diffraction", *Phys. Rev. D* **59** (1998) 014017, arXiv:hep-ph/9807513.

[49] E. Iancu, K. Itakura, and S. Munier, "Saturation and BFKL dynamics in the HERA data at small x", *Phys. Lett. B* **590** (2004) 199–208, arXiv:hep-ph/0310338.

[50] **ALICE** Collaboration, S. Acharya *et al.*, "The ALICE experiment: a journey through QCD", *Eur. Phys. J. C* **84** (2024) 813, arXiv:2211.04384 [nucl-ex].

[51] **ALICE** Collaboration, B. Abelev *et al.*, "Upgrade of the ALICE Experiment: Letter Of Intent", *J. Phys. G* **41** (2014) 087001.

A The ALICE Collaboration

S. Acharya [127], A. Agarwal[135], G. Aglieri Rinella [32], L. Aglietta [24], M. Agnello [29], N. Agrawal [25],
Z. Ahammed [135], S. Ahmad [15], S.U. Ahn [71], I. Ahuja [37], A. Akindinov [140], V. Akishina[38],
M. Al-Turany [97], D. Aleksandrov [140], B. Alessandro [56], H.M. Alfanda [6], R. Alfaro Molina [67],
B. Ali [15], A. Alici [25], N. Alizadehvandchali [116], A. Alkin [104], J. Alme [20], G. Alocco [24,52], T. Alt [64],
A.R. Altamura [50], I. Altsybeev [95], J.R. Alvarado [44], C.O.R. Alvarez[44], M.N. Anaam [6], C. Andrei [45],
N. Andreou [115], A. Andronic [126], E. Andronov [140], V. Anguelov [94], F. Antinori [54], P. Antonioli [51],
N. Apadula [74], L. Aphecetche [103], H. Appelshäuser [64], C. Arata [73], S. Arcelli [25], R. Arnaldi [56],
J.G.M.C.A. Arneiro [110], I.C. Arsene [19], M. Arslandok [138], A. Augustinus [32], R. Averbeck [97],
D. Averyanov [140], M.D. Azmi [15], H. Baba[124], A. Badalà [53], J. Bae [104], Y.W. Baek [40], X. Bai [120],
R. Bailhache [64], Y. Bailung [48], R. Bala [91], A. Balbino [29], A. Baldisseri [130], B. Balis [2], Z. Banoo [91],
V. Barbasova[37], F. Barile [31], L. Barioglio [56], M. Barlou[78], B. Barman[41], G.G. Barnaföldi [46],
L.S. Barnby [115], E. Barreau [103], V. Barret [127], L. Barreto [110], C. Bartels [119], K. Barth [32],
E. Bartsch [64], N. Bastid [127], S. Basu [75], G. Batigne [103], D. Battistini [95], B. Batyunya [141], D. Bauri[47],
J.L. Bazo Alba [101], I.G. Bearden [83], C. Beattie [138], P. Becht [97], D. Behera [48], I. Belikov [129],
A.D.C. Bell Hechavarria [126], F. Bellini [25], R. Bellwied [116], S. Belokurova [140], L.G.E. Beltran [109],
Y.A.V. Beltran [44], G. Bencedi [46], A. Bensaoula[116], S. Beole [24], Y. Berdnikov [140], A. Berdnikova [94],
L. Bergmann [94], M.G. Besoiu [63], L. Betev [32], P.P. Bhaduri [135], A. Bhasin [91], B. Bhattacharjee [41],
L. Bianchi [24], J. Bielčík [35], J. Bielčíková [86], A.P. Bigot [129], A. Bilandzic [95], G. Biro [46], S. Biswas [4],
N. Bize [103], J.T. Blair [108], D. Blau [140], M.B. Blidaru [97], N. Bluhme[38], C. Blume [64], G. Boca [21,55],
F. Bock [87], T. Bodova [20], J. Bok [16], L. Boldizsár [46], M. Bombara [37], P.M. Bond [32], G. Bonomi [134,55],
H. Borel [130], A. Borissov [140], A.G. Borquez Carcamo [94], E. Botta [24], Y.E.M. Bouziani [64],
L. Bratrud [64], P. Braun-Munzinger [97], M. Bregant [110], M. Broz [35], G.E. Bruno [96,31],
V.D. Buchakchiev [36], M.D. Buckland [85], D. Budnikov [140], H. Buesching [64], S. Bufalino [29],
P. Buhler [102], N. Burmasov [140], Z. Buthelezi [68,123], A. Bylinkin [20], S.A. Bysiak[107], J.C. Cabanillas
Noris [109], M.F.T. Cabrera[116], M. Cai [6], H. Caines [138], A. Caliva [28], E. Calvo Villar [101],
J.M.M. Camacho [109], P. Camerini [23], F.D.M. Canedo [110], S.L. Cantway [138], M. Carabas [113],
A.A. Carballo [32], F. Carnesecchi [32], R. Caron [128], L.A.D. Carvalho [110], J. Castillo Castellanos [130],
M. Castoldi [32], F. Catalano [32], S. Cattaruzzi [23], C. Ceballos Sanchez [7], R. Cerri [24], I. Chakaberia [74],
P. Chakraborty [136], S. Chandra [135], S. Chapeland [32], M. Chartier [119], S. Chattopadhay[135],
S. Chattopadhyay [135], S. Chattopadhyay [99], M. Chen[39], T. Cheng [6], C. Cheshkov [128], V. Chibante
Barroso [32], D.D. Chinellato [102], E.S. Chizzali [II,95], J. Cho [58], S. Cho [58], P. Chochula [32],
Z.A. Chochulska[136], D. Choudhury[41], P. Christakoglou [84], C.H. Christensen [83], P. Christiansen [75],
T. Chujo [125], M. Ciacco [29], C. Cicalo [52], M.R. Ciupek[97], G. Clai[III,51], F. Colamaria [50], J.S. Colburn[100],
D. Colella [31], A. Colelli[31], M. Colocci [25], M. Concas [32], G. Conesa Balbastre [73], Z. Conesa del
Valle [131], G. Contin [23], J.G. Contreras [35], M.L. Coquet [103], P. Cortese [133,56], M.R. Cosentino [112],
F. Costa [32], S. Costanza [21,55], C. Cot [131], P. Crochet [127], R. Cruz-Torres [74], M.M. Czarnynoga[136],
A. Dainese [54], G. Dange[38], M.C. Danisch [94], A. Danu [63], P. Das [80], S. Das [4], A.R. Dash [126],
S. Dash [47], A. De Caro [28], G. de Cataldo [50], J. de Cuveland[38], A. De Falco [22], D. De Gruttola [28], N. De
Marco [56], C. De Martin [23], S. De Pasquale [28], R. Deb [134], R. Del Grande [95], L. Dello Stritto [32],
W. Deng [6], K.C. Devereaux[18], P. Dhankher [18], D. Di Bari [31], A. Di Mauro [32], B. Di Ruzza [132],
B. Diab [130], R.A. Diaz [141,7], T. Dietel [114], Y. Ding [6], J. Ditzel [64], R. Divià [32], Ø. Djuvsland[20],
U. Dmitrieva [140], A. Dobrin [63], B. Dönigus [64], J.M. Dubinski [136], A. Dubla [97], P. Dupieux [127],
N. Dzalaiova[13], T.M. Eder [126], R.J. Ehlers [74], F. Eisenhut [64], R. Ejima [92], D. Elia [50], B. Erazmus [103],
F. Ercolessi [25], B. Espagnon [131], G. Eulisse [32], D. Evans [100], S. Evdokimov [140], L. Fabbietti [95],
M. Faggin [23], J. Faivre [73], F. Fan [6], W. Fan [74], A. Fantoni [49], M. Fasel [87], A. Feliciello [56],
G. Feofilov [140], A. Fernández Téllez [44], L. Ferrandi [110], M.B. Ferrer [32], A. Ferrero [130],
C. Ferrero [IV,56], A. Ferretti [24], V.J.G. Feuillard [94], V. Filova [35], D. Finogeev [140], F.M. Fionda [52],
E. Flatland[32], F. Flor [138,116], A.N. Flores [108], S. Foertsch [68], I. Fokin [94], S. Fokin [140], U. Follo [IV,56],
E. Fragiacomo [57], E. Frajna [46], U. Fuchs [32], N. Funicello [28], C. Furget [73], A. Furs [140],
T. Fusayasu [98], J.J. Gaardhøje [83], M. Gagliardi [24], A.M. Gago [101], T. Gahlaut[47], C.D. Galvan [109],
S. Gami[80], D.R. Gangadharan [116], P. Ganoti [78], C. Garabatos [97], J.M. Garcia[44], T. García Chávez [44],
E. Garcia-Solis [9], C. Gargiulo [32], P. Gasik [97], H.M. Gaur[38], A. Gautam [118], M.B. Gay Ducati [66],
M. Germain [103], R.A. Gernhaeuser[95], C. Ghosh[135], M. Giacalone [51], G. Gioachin [29], S.K. Giri[135],
P. Giubellino [97,56], P. Giubilato [27], A.M.C. Glaenzer [130], P. Glässel [94], E. Glimos [122], D.J.Q. Goh[76],
V. Gonzalez [137], P. Gordeev [140], M. Gorgon [2], K. Goswami [48], S. Gotovac[33], V. Grabski [67],

L.K. Graczykowski [136], E. Grecka [86], A. Grelli [59], C. Grigoras [32], V. Grigoriev [140], S. Grigoryan [141,1], F. Grosa [32], J.F. Grosse-Oetringhaus [32], R. Grosso [97], D. Grund [35], N.A. Grunwald[94], G.G. Guardiano [111], R. Guernane [73], M. Guilbaud [103], K. Gulbrandsen [83], J.J.W.K. Gumprecht[102], T. Gündem [64], T. Gunji [124], W. Guo [6], A. Gupta [91], R. Gupta [91], R. Gupta [48], K. Gwizdziel [136], L. Gyulai [46], C. Hadjidakis [131], F.U. Haider [91], S. Haidlova [35], M. Haldar[4], H. Hamagaki [76], Y. Han [139], B.G. Hanley [137], R. Hannigan [108], J. Hansen [75], M.R. Haque [97], J.W. Harris [138], A. Harton [9], M.V. Hartung [64], H. Hassan [117], D. Hatzifotiadou [51], P. Hauer [42], L.B. Havener [138], E. Hellbär [32], H. Helstrup [34], M. Hemmer [64], T. Herman [35], S.G. Hernandez[116], G. Herrera Corral [8], S. Herrmann [128], K.F. Hetland [34], B. Heybeck [64], H. Hillemanns [32], B. Hippolyte [129], I.P.M. Hobus[84], F.W. Hoffmann [70], B. Hofman [59], G.H. Hong [139], M. Horst [95], A. Horzyk [2], Y. Hou [6], P. Hristov [32], P. Huhn[64], L.M. Huhta [117], T.J. Humanic [88], A. Hutson [116], D. Hutter [38], M.C. Hwang [18], R. Ilkaev[140], M. Inaba [125], G.M. Innocenti [32], M. Ippolitov [140], A. Isakov [84], T. Isidori [118], M.S. Islam [99], S. Iurchenko[140], M. Ivanov [13], M. Ivanov [97], V. Ivanov [140], K.E. Iversen [75], M. Jablonski [2], B. Jacak [18,74], N. Jacazio [25], P.M. Jacobs [74], S. Jadlovska [106], J. Jadlovsky[106], S. Jaelani [82], C. Jahnke [110], M.J. Jakubowska [136], M.A. Janik [136], T. Janson[70], S. Ji [16], S. Jia [10], T. Jiang [10], A.A.P. Jimenez [65], F. Jonas [74], D.M. Jones [119], J.M. Jowett [32,97], J. Jung [64], M. Jung [64], A. Junique [32], A. Jusko [100], J. Kaewjai[105], P. Kalinak [60], A. Kalweit [32], A. Karasu Uysal [V,72], D. Karatovic [89], N. Karatzenis[100], O. Karavichev [140], T. Karavicheva [140], E. Karpechev [140], M.J. Karwowska [32,136], U. Kebschull [70], M. Keil [32], B. Ketzer [42], J. Keul [64], S.S. Khade [48], A.M. Khan [120], S. Khan [15], A. Khanzadeev [140], Y. Kharlov [140], A. Khatun [118], A. Khuntia [35], Z. Khuranova [64], B. Kileng [34], B. Kim [104], C. Kim [16], D.J. Kim [117], E.J. Kim [69], J. Kim [139], J. Kim [58], J. Kim [32,69], M. Kim [18], S. Kim [17], T. Kim [139], K. Kimura [92], A. Kirkova[36], S. Kirsch [64], I. Kisel [38], S. Kiselev [140], A. Kisiel [136], J.P. Kitowski [2], J.L. Klay [5], J. Klein [32], S. Klein [74], C. Klein-Bösing [126], M. Kleiner [64], T. Klemenz [95], A. Kluge [32], C. Kobdaj [105], R. Kohara[124], T. Kollegger[97], A. Kondratyev [141], N. Kondratyeva [140], J. Konig [64], S.A. Konigstorfer [95], P.J. Konopka [32], G. Kornakov [136], M. Korwieser [95], S.D. Koryciak [2], C. Koster[84], A. Kotliarov [86], N. Kovacic[89], V. Kovalenko [140], M. Kowalski [107], V. Kozhuharov [36], G. Kozlov[38], I. Králik [60], A. Kravčáková [37], L. Krcal [32,38], M. Krivda [100,60], F. Krizek [86], K. Krizkova Gajdosova [32], C. Krug [66], M. Krüger [64], D.M. Krupova [35], E. Kryshen [140], V. Kučera [58], C. Kuhn [129], P.G. Kuijer [84], T. Kumaoka[125], D. Kumar[135], L. Kumar [90], N. Kumar[90], S. Kumar [50], S. Kundu [32], P. Kurashvili [79], A. Kurepin [140], A.B. Kurepin [140], A. Kuryakin [140], S. Kushpil [86], V. Kuskov [140], M. Kutyla[136], A. Kuznetsov[141], M.J. Kweon [58], Y. Kwon [139], S.L. La Pointe [38], P. La Rocca [26], A. Lakrathok[105], M. Lamanna [32], A.R. Landou [73], R. Langoy [121], P. Larionov [32], E. Laudi [32], L. Lautner [32,95], R.A.N. Laveaga[109], R. Lavicka [102], R. Lea [134,55], H. Lee [104], I. Legrand [45], G. Legras [126], J. Lehrbach [38], A.M. Lejeune[35], T.M. Lelek[2], R.C. Lemmon [I,85], I. León Monzón [109], M.M. Lesch [95], E.D. Lesser [18], P. Lévai [46], M. Li[6], P. Li[10], X. Li[10], B.E. Liang-gilman [18], J. Lien [121], R. Lietava [100], I. Likmeta [116], B. Lim [24], S.H. Lim [16], V. Lindenstruth [38], C. Lippmann [97], D.H. Liu [6], J. Liu [119], G.S.S. Liveraro [111], I.M. Lofnes [20], C. Loizides [87], S. Lokos [107], J. Lömker [59], X. Lopez [127], E. López Torres [7], C. Lotteau[128], P. Lu [97,120], Z. Lu [10], F.V. Lugo [67], J.R. Luhder [126], M. Lunardon [27], G. Luparello [57], Y.G. Ma [39], M. Mager [32], A. Maire [129], E.M. Majerz[2], M.V. Makariev [36], M. Malaev [140], G. Malfattore [25], N.M. Malik [91], S.K. Malik [91], L. Malinina [I,VIII,141], D. Mallick [131], N. Mallick [48], G. Mandaglio [30,53], S.K. Mandal [79], A. Manea [63], V. Manko [140], F. Manso [127], V. Manzari [50], Y. Mao [6], R.W. Marcjan [2], G.V. Margagliotti [23], A. Margotti [51], A. Marín [97], C. Markert [108], C.F.B. Marquez[31], P. Martinengo [32], M.I. Martínez [44], G. Martínez García [103], M.P.P. Martins [110], S. Masciocchi [97], M. Masera [24], A. Masoni [52], L. Massacrier [131], O. Massen [59], A. Mastroserio [132,50], O. Matonoha [75], S. Mattiazzo [27], A. Matyja [107], F. Mazzaschi [32,24], M. Mazzilli [116], Y. Melikyan [43], M. Melo [110], A. Menchaca-Rocha [67], J.E.M. Mendez [65], E. Meninno [102], A.S. Menon [116], M.W. Menzel[32,94], M. Meres [13], Y. Miake[125], L. Micheletti [32], D. Mihai[113], D.L. Mihaylov [95], K. Mikhaylov [141,140], N. Minafra [118], D. Miśkowiec [97], A. Modak [134], B. Mohanty[80], M. Mohisin Khan [VI,15], M.A. Molander [43], S. Monira [136], C. Mordasini [117], D.A. Moreira De Godoy [126], I. Morozov [140], A. Morsch [32], T. Mrnjavac [32], V. Muccifora [49], S. Muhuri [135], J.D. Mulligan [74], A. Mulliri [22], M.G. Munhoz [110], R.H. Munzer [64], H. Murakami [124], S. Murray [114], L. Musa [32], J. Musinsky [60], J.W. Myrcha [136], B. Naik [123], A.I. Nambrath [18], B.K. Nandi [47], R. Nania [51], E. Nappi [50], A.F. Nassirpour [17], V. Nastase[113], A. Nath [94], S. Nath[135], C. Nattrass [122], M.N. Naydenov [36], A. Neagu[19], A. Negru[113], E. Nekrasova[140], L. Nellen [65], R. Nepeivoda [75], S. Nese [19], N. Nicassio [50], B.S. Nielsen [83], E.G. Nielsen [83], S. Nikolaev [140], S. Nikulin [140], V. Nikulin [140], F. Noferini [51], S. Noh [12], P. Nomokonov [141],

J. Norman [119], N. Novitzky [87], P. Nowakowski [136], A. Nyanin [140], J. Nystrand [20], S. Oh [17],
A. Ohlson [75], V.A. Okorokov [140], J. Oleniacz [136], A. Onnerstad [117], C. Oppedisano [56], A. Ortiz
Velasquez [65], J. Otwinowski [107], M. Oya[92], K. Oyama [76], Y. Pachmayer [94], S. Padhan [47],
D. Pagano [134,55], G. Paić [65], S. Paisano-Guzmán [44], A. Palasciano [50], I. Panasenko[75], S. Panebianco [130],
C. Pantouvakis [27], H. Park [125], H. Park [104], J. Park [125], J.E. Parkkila [32], Y. Patley [47], R.N. Patra[50],
B. Paul [135], H. Pei [6], T. Peitzmann [59], X. Peng [11], M. Pennisi [24], S. Perciballi [24], D. Peresunko [140],
G.M. Perez [7], Y. Pestov[140], M.T. Petersen[83], V. Petrov [140], M. Petrovici [45], S. Piano [57], M. Pikna [13],
P. Pillot [103], O. Pinazza [51,32], L. Pinsky [116], C. Pinto [95], S. Pisano [49], M. Płoskoń [74], M. Planinic[89],
F. Pliquett[64], D.K. Plociennik [2], M.G. Poghosyan [87], B. Polichtchouk [140], S. Politano [29], N. Poljak [89],
A. Pop [45], S. Porteboeuf-Houssais [127], V. Pozdniakov [I,141], I.Y. Pozos [44], K.K. Pradhan [48],
S.K. Prasad [4], S. Prasad [48], R. Preghenella [51], F. Prino [56], C.A. Pruneau [137], I. Pshenichnov [140],
M. Puccio [32], S. Pucillo [24], S. Qiu [84], L. Quaglia [24], A.M.K. Radhakrishnan[48], S. Ragoni [14],
A. Rai [138], A. Rakotozafindrabe [130], L. Ramello [133,56], F. Rami [129], M. Rasa [26], S.S. Räsänen [43],
R. Rath [51], M.P. Rauch [20], I. Ravasenga [32], K.F. Read [87,122], C. Reckziegel [112], A.R. Redelbach [38],
K. Redlich [VII,79], C.A. Reetz [97], H.D. Regules-Medel[44], A. Rehman[20], F. Reidt [32], H.A. Reme-Ness [34],
K. Reygers [94], A. Riabov [140], V. Riabov [140], R. Ricci [28], M. Richter [20], A.A. Riedel [95],
W. Riegler [32], A.G. Riffero [24], M. Rignanese [27], C. Ripoli[28], C. Ristea [63], M.V. Rodriguez [32],
M. Rodríguez Cahuantzi [44], S.A. Rodríguez Ramírez [44], K. Røed [19], R. Rogalev [140], E. Rogochaya [141],
T.S. Rogoschinski [64], D. Rohr [32], D. Röhrich [20], S. Rojas Torres [35], P.S. Rokita [136], G. Romanenko [25],
F. Ronchetti [32], E.D. Rosas[65], K. Roslon [136], A. Rossi [54], A. Roy [48], S. Roy [47], N. Rubini [51,25],
J.A. Rudolph[84], D. Ruggiano [136], R. Rui [23], P.G. Russek [2], R. Russo [84], A. Rustamov [81],
E. Ryabinkin [140], Y. Ryabov [140], A. Rybicki [107], J. Ryu [16], W. Rzesa [136], B. Sabiu[51], S. Sadovsky [140],
J. Saetre [20], K. Šafařík [35], S. Saha [80], B. Sahoo [48], R. Sahoo [48], S. Sahoo[61], D. Sahu [48], P.K. Sahu [61],
J. Saini [135], K. Sajdakova[37], S. Sakai [125], M.P. Salvan [97], S. Sambyal [91], D. Samitz [102], I. Sanna [32,95],
T.B. Saramela [110], D. Sarkar [83], P. Sarma [41], V. Sarritzu [22], V.M. Sarti [95], M.H.P. Sas [32], S. Sawan [80],
E. Scapparone [51], J. Schambach [87], H.S. Scheid [64], C. Schiaua [45], R. Schicker [94], F. Schlepper [94],
A. Schmah[97], C. Schmidt [97], H.R. Schmidt[93], M.O. Schmidt [32], M. Schmidt[93], N.V. Schmidt [87],
A.R. Schmier [122], R. Schotter [102,129], A. Schröter [38], J. Schukraft [32], K. Schweda [97], G. Scioli [25],
E. Scomparin [56], J.E. Seger [14], Y. Sekiguchi[124], D. Sekihata [124], M. Selina [84], I. Selyuzhenkov [97],
S. Senyukov [129], J.J. Seo [94], D. Serebryakov [140], L. Serkin [65], L. Šerkšnytė [95], A. Sevcenco [63],
T.J. Shaba [68], A. Shabetai [103], R. Shahoyan[32], A. Shangaraev [140], B. Sharma [91], D. Sharma [47],
H. Sharma [54], M. Sharma [91], S. Sharma [76], S. Sharma [91], U. Sharma [91], A. Shatat [131], O. Sheibani[116],
K. Shigaki [92], M. Shimomura[77], J. Shin[12], S. Shirinkin [140], Q. Shou [39], Y. Sibiriak [140], S. Siddhanta [52],
T. Siemiarczuk [79], T.F. Silva [110], D. Silvermyr [75], T. Simantathammakul[105], R. Simeonov [36], B. Singh[91],
B. Singh [95], K. Singh [48], R. Singh [80], R. Singh [91], R. Singh [97], S. Singh [15], V.K. Singh [135],
V. Singhal [135], T. Sinha [99], B. Sitar [13], M. Sitta [133,56], T.B. Skaali[19], G. Skorodumovs [94],
N. Smirnov [138], R.J.M. Snellings [59], E.H. Solheim [19], J. Song [16], C. Sonnabend [32,97],
J.M. Sonneveld [84], F. Soramel [27], A.B. Soto-hernandez [88], R. Spijkers [84], I. Sputowska [107], J. Staa [75],
J. Stachel [94], I. Stan [63], P.J. Steffanic [122], T. Stellhorn[126], S.F. Stiefelmaier [94], D. Stocco [103],
I. Storehaug [19], N.J. Strangmann [64], P. Stratmann [126], S. Strazzi [25], A. Sturniolo [30,53], C.P. Stylianidis[84],
A.A.P. Suaide [110], C. Suire [131], M. Sukhanov [140], M. Suljic [32], R. Sultanov [140], V. Sumberia [91],
S. Sumowidagdo [82], M. Szymkowski [136], S.F. Taghavi [95], G. Taillepied [97], J. Takahashi [111],
G.J. Tambave [80], S. Tang [6], Z. Tang [120], J.D. Tapia Takaki [118], N. Tapus[113], L.A. Tarasovicova [37],
M.G. Tarzila [45], G.F. Tassielli [31], A. Tauro [32], A. Tavira García [131], G. Tejeda Muñoz [44], L. Terlizzi [24],
C. Terrevoli [50], S. Thakur [4], D. Thomas [108], A. Tikhonov [140], N. Tiltmann [32,126], A.R. Timmins [116],
M. Tkacik[106], T. Tkacik [106], A. Toia [64], R. Tokumoto[92], S. Tomassini[25], K. Tomohiro[92], N. Topilskaya [140],
M. Toppi [49], V.V. Torres [103], A.G. Torres Ramos [31], A. Trifiró [30,53], T. Triloki[96], A.S. Triolo [32,30,53],
S. Tripathy [32], T. Tripathy [47], S. Trogolo [24], V. Trubnikov [3], W.H. Trzaska [117], T.P. Trzcinski [136],
C. Tsolanta[19], R. Tu[39], A. Tumkin [140], R. Turrisi [54], T.S. Tveter [19], K. Ullaland [20], B. Ulukutlu [95],
S. Upadhyaya [107], A. Uras [128], M. Urioni [134], G.L. Usai [22], M. Vala[37], N. Valle [55], L.V.R. van
Doremalen[59], M. van Leeuwen [84], C.A. van Veen [94], R.J.G. van Weelden [84], P. Vande Vyvre [32],
D. Varga [46], Z. Varga [46], P. Vargas Torres[65], M. Vasileiou [78], A. Vasiliev [I,140], O. Vázquez Doce [49],
O. Vazquez Rueda [116], V. Vechernin [140], E. Vercellin [24], S. Vergara Limón[44], R. Verma [47],
L. Vermunt [97], R. Vértesi [46], M. Verweij [59], L. Vickovic[33], Z. Vilakazi[123], O. Villalobos Baillie [100],
A. Villani [23], A. Vinogradov [140], T. Virgili [28], M.M.O. Virta [117], A. Vodopyanov [141], B. Volkel [32],
M.A. Völkl [94], S.A. Voloshin [137], G. Volpe [31], B. von Haller [32], I. Vorobyev [32], N. Vozniuk [140],

J. Vrláková [37], J. Wan[39], C. Wang [39], D. Wang[39], Y. Wang [39], Y. Wang [6], Z. Wang [39],
A. Wegrzynek [32], F.T. Weiglhofer[38], S.C. Wenzel [32], J.P. Wessels [126], J. Wiechula [64], J. Wikne [19],
G. Wilk [79], J. Wilkinson [97], G.A. Willems [126], B. Windelband [94], M. Winn [130], J.R. Wright [108],
W. Wu[39], Y. Wu [120], Z. Xiong[120], R. Xu [6], A. Yadav [42], A.K. Yadav [135], Y. Yamaguchi [92], S. Yang[20],
S. Yano [92], E.R. Yeats[18], Z. Yin [6], I.-K. Yoo [16], J.H. Yoon [58], H. Yu[12], S. Yuan[20], A. Yuncu [94],
V. Zaccolo [23], C. Zampolli [32], F. Zanone [94], N. Zardoshti [32], A. Zarochentsev [140], P. Závada [62],
N. Zaviyalov[140], M. Zhalov [140], B. Zhang [94,6], C. Zhang [130], L. Zhang [39], M. Zhang [127,6], M. Zhang [6],
S. Zhang [39], X. Zhang [6], Y. Zhang[120], Z. Zhang [6], M. Zhao [10], V. Zherebchevskii [140], Y. Zhi[10],
D. Zhou [6], Y. Zhou [83], J. Zhu [54,6], S. Zhu[120], Y. Zhu[6], S.C. Zugravel [56], N. Zurlo [134,55]

Affiliation Notes

[I] Deceased
[II] Also at: Max-Planck-Institut fur Physik, Munich, Germany
[III] Also at: Italian National Agency for New Technologies, Energy and Sustainable Economic Development (ENEA), Bologna, Italy
[IV] Also at: Dipartimento DET del Politecnico di Torino, Turin, Italy
[V] Also at: Yildiz Technical University, Istanbul, Türkiye
[VI] Also at: Department of Applied Physics, Aligarh Muslim University, Aligarh, India
[VII] Also at: Institute of Theoretical Physics, University of Wroclaw, Poland
[VIII] Also at: An institution covered by a cooperation agreement with CERN

Collaboration Institutes

[1] A.I. Alikhanyan National Science Laboratory (Yerevan Physics Institute) Foundation, Yerevan, Armenia
[2] AGH University of Krakow, Cracow, Poland
[3] Bogolyubov Institute for Theoretical Physics, National Academy of Sciences of Ukraine, Kiev, Ukraine
[4] Bose Institute, Department of Physics and Centre for Astroparticle Physics and Space Science (CAPSS), Kolkata, India
[5] California Polytechnic State University, San Luis Obispo, California, United States
[6] Central China Normal University, Wuhan, China
[7] Centro de Aplicaciones Tecnológicas y Desarrollo Nuclear (CEADEN), Havana, Cuba
[8] Centro de Investigación y de Estudios Avanzados (CINVESTAV), Mexico City and Mérida, Mexico
[9] Chicago State University, Chicago, Illinois, United States
[10] China Institute of Atomic Energy, Beijing, China
[11] China University of Geosciences, Wuhan, China
[12] Chungbuk National University, Cheongju, Republic of Korea
[13] Comenius University Bratislava, Faculty of Mathematics, Physics and Informatics, Bratislava, Slovak Republic
[14] Creighton University, Omaha, Nebraska, United States
[15] Department of Physics, Aligarh Muslim University, Aligarh, India
[16] Department of Physics, Pusan National University, Pusan, Republic of Korea
[17] Department of Physics, Sejong University, Seoul, Republic of Korea
[18] Department of Physics, University of California, Berkeley, California, United States
[19] Department of Physics, University of Oslo, Oslo, Norway
[20] Department of Physics and Technology, University of Bergen, Bergen, Norway
[21] Dipartimento di Fisica, Università di Pavia, Pavia, Italy
[22] Dipartimento di Fisica dell'Università and Sezione INFN, Cagliari, Italy
[23] Dipartimento di Fisica dell'Università and Sezione INFN, Trieste, Italy
[24] Dipartimento di Fisica dell'Università and Sezione INFN, Turin, Italy
[25] Dipartimento di Fisica e Astronomia dell'Università and Sezione INFN, Bologna, Italy
[26] Dipartimento di Fisica e Astronomia dell'Università and Sezione INFN, Catania, Italy
[27] Dipartimento di Fisica e Astronomia dell'Università and Sezione INFN, Padova, Italy
[28] Dipartimento di Fisica 'E.R. Caianiello' dell'Università and Gruppo Collegato INFN, Salerno, Italy
[29] Dipartimento DISAT del Politecnico and Sezione INFN, Turin, Italy
[30] Dipartimento di Scienze MIFT, Università di Messina, Messina, Italy
[31] Dipartimento Interateneo di Fisica 'M. Merlin' and Sezione INFN, Bari, Italy

[32] European Organization for Nuclear Research (CERN), Geneva, Switzerland
[33] Faculty of Electrical Engineering, Mechanical Engineering and Naval Architecture, University of Split, Split, Croatia
[34] Faculty of Engineering and Science, Western Norway University of Applied Sciences, Bergen, Norway
[35] Faculty of Nuclear Sciences and Physical Engineering, Czech Technical University in Prague, Prague, Czech Republic
[36] Faculty of Physics, Sofia University, Sofia, Bulgaria
[37] Faculty of Science, P.J. Šafárik University, Košice, Slovak Republic
[38] Frankfurt Institute for Advanced Studies, Johann Wolfgang Goethe-Universität Frankfurt, Frankfurt, Germany
[39] Fudan University, Shanghai, China
[40] Gangneung-Wonju National University, Gangneung, Republic of Korea
[41] Gauhati University, Department of Physics, Guwahati, India
[42] Helmholtz-Institut für Strahlen- und Kernphysik, Rheinische Friedrich-Wilhelms-Universität Bonn, Bonn, Germany
[43] Helsinki Institute of Physics (HIP), Helsinki, Finland
[44] High Energy Physics Group, Universidad Autónoma de Puebla, Puebla, Mexico
[45] Horia Hulubei National Institute of Physics and Nuclear Engineering, Bucharest, Romania
[46] HUN-REN Wigner Research Centre for Physics, Budapest, Hungary
[47] Indian Institute of Technology Bombay (IIT), Mumbai, India
[48] Indian Institute of Technology Indore, Indore, India
[49] INFN, Laboratori Nazionali di Frascati, Frascati, Italy
[50] INFN, Sezione di Bari, Bari, Italy
[51] INFN, Sezione di Bologna, Bologna, Italy
[52] INFN, Sezione di Cagliari, Cagliari, Italy
[53] INFN, Sezione di Catania, Catania, Italy
[54] INFN, Sezione di Padova, Padova, Italy
[55] INFN, Sezione di Pavia, Pavia, Italy
[56] INFN, Sezione di Torino, Turin, Italy
[57] INFN, Sezione di Trieste, Trieste, Italy
[58] Inha University, Incheon, Republic of Korea
[59] Institute for Gravitational and Subatomic Physics (GRASP), Utrecht University/Nikhef, Utrecht, Netherlands
[60] Institute of Experimental Physics, Slovak Academy of Sciences, Košice, Slovak Republic
[61] Institute of Physics, Homi Bhabha National Institute, Bhubaneswar, India
[62] Institute of Physics of the Czech Academy of Sciences, Prague, Czech Republic
[63] Institute of Space Science (ISS), Bucharest, Romania
[64] Institut für Kernphysik, Johann Wolfgang Goethe-Universität Frankfurt, Frankfurt, Germany
[65] Instituto de Ciencias Nucleares, Universidad Nacional Autónoma de México, Mexico City, Mexico
[66] Instituto de Física, Universidade Federal do Rio Grande do Sul (UFRGS), Porto Alegre, Brazil
[67] Instituto de Física, Universidad Nacional Autónoma de México, Mexico City, Mexico
[68] iThemba LABS, National Research Foundation, Somerset West, South Africa
[69] Jeonbuk National University, Jeonju, Republic of Korea
[70] Johann-Wolfgang-Goethe Universität Frankfurt Institut für Informatik, Fachbereich Informatik und Mathematik, Frankfurt, Germany
[71] Korea Institute of Science and Technology Information, Daejeon, Republic of Korea
[72] KTO Karatay University, Konya, Turkey
[73] Laboratoire de Physique Subatomique et de Cosmologie, Université Grenoble-Alpes, CNRS-IN2P3, Grenoble, France
[74] Lawrence Berkeley National Laboratory, Berkeley, California, United States
[75] Lund University Department of Physics, Division of Particle Physics, Lund, Sweden
[76] Nagasaki Institute of Applied Science, Nagasaki, Japan
[77] Nara Women's University (NWU), Nara, Japan
[78] National and Kapodistrian University of Athens, School of Science, Department of Physics , Athens, Greece
[79] National Centre for Nuclear Research, Warsaw, Poland
[80] National Institute of Science Education and Research, Homi Bhabha National Institute, Jatni, India
[81] National Nuclear Research Center, Baku, Azerbaijan
[82] National Research and Innovation Agency - BRIN, Jakarta, Indonesia

[83] Niels Bohr Institute, University of Copenhagen, Copenhagen, Denmark
[84] Nikhef, National institute for subatomic physics, Amsterdam, Netherlands
[85] Nuclear Physics Group, STFC Daresbury Laboratory, Daresbury, United Kingdom
[86] Nuclear Physics Institute of the Czech Academy of Sciences, Husinec-Řež, Czech Republic
[87] Oak Ridge National Laboratory, Oak Ridge, Tennessee, United States
[88] Ohio State University, Columbus, Ohio, United States
[89] Physics department, Faculty of science, University of Zagreb, Zagreb, Croatia
[90] Physics Department, Panjab University, Chandigarh, India
[91] Physics Department, University of Jammu, Jammu, India
[92] Physics Program and International Institute for Sustainability with Knotted Chiral Meta Matter (SKCM2), Hiroshima University, Hiroshima, Japan
[93] Physikalisches Institut, Eberhard-Karls-Universität Tübingen, Tübingen, Germany
[94] Physikalisches Institut, Ruprecht-Karls-Universität Heidelberg, Heidelberg, Germany
[95] Physik Department, Technische Universität München, Munich, Germany
[96] Politecnico di Bari and Sezione INFN, Bari, Italy
[97] Research Division and ExtreMe Matter Institute EMMI, GSI Helmholtzzentrum für Schwerionenforschung GmbH, Darmstadt, Germany
[98] Saga University, Saga, Japan
[99] Saha Institute of Nuclear Physics, Homi Bhabha National Institute, Kolkata, India
[100] School of Physics and Astronomy, University of Birmingham, Birmingham, United Kingdom
[101] Sección Física, Departamento de Ciencias, Pontificia Universidad Católica del Perú, Lima, Peru
[102] Stefan Meyer Institut für Subatomare Physik (SMI), Vienna, Austria
[103] SUBATECH, IMT Atlantique, Nantes Université, CNRS-IN2P3, Nantes, France
[104] Sungkyunkwan University, Suwon City, Republic of Korea
[105] Suranaree University of Technology, Nakhon Ratchasima, Thailand
[106] Technical University of Košice, Košice, Slovak Republic
[107] The Henryk Niewodniczanski Institute of Nuclear Physics, Polish Academy of Sciences, Cracow, Poland
[108] The University of Texas at Austin, Austin, Texas, United States
[109] Universidad Autónoma de Sinaloa, Culiacán, Mexico
[110] Universidade de São Paulo (USP), São Paulo, Brazil
[111] Universidade Estadual de Campinas (UNICAMP), Campinas, Brazil
[112] Universidade Federal do ABC, Santo Andre, Brazil
[113] Universitatea Nationala de Stiinta si Tehnologie Politehnica Bucuresti, Bucharest, Romania
[114] University of Cape Town, Cape Town, South Africa
[115] University of Derby, Derby, United Kingdom
[116] University of Houston, Houston, Texas, United States
[117] University of Jyväskylä, Jyväskylä, Finland
[118] University of Kansas, Lawrence, Kansas, United States
[119] University of Liverpool, Liverpool, United Kingdom
[120] University of Science and Technology of China, Hefei, China
[121] University of South-Eastern Norway, Kongsberg, Norway
[122] University of Tennessee, Knoxville, Tennessee, United States
[123] University of the Witwatersrand, Johannesburg, South Africa
[124] University of Tokyo, Tokyo, Japan
[125] University of Tsukuba, Tsukuba, Japan
[126] Universität Münster, Institut für Kernphysik, Münster, Germany
[127] Université Clermont Auvergne, CNRS/IN2P3, LPC, Clermont-Ferrand, France
[128] Université de Lyon, CNRS/IN2P3, Institut de Physique des 2 Infinis de Lyon, Lyon, France
[129] Université de Strasbourg, CNRS, IPHC UMR 7178, F-67000 Strasbourg, France, Strasbourg, France
[130] Université Paris-Saclay, Centre d'Etudes de Saclay (CEA), IRFU, Départment de Physique Nucléaire (DPhN), Saclay, France
[131] Université Paris-Saclay, CNRS/IN2P3, IJCLab, Orsay, France
[132] Università degli Studi di Foggia, Foggia, Italy
[133] Università del Piemonte Orientale, Vercelli, Italy
[134] Università di Brescia, Brescia, Italy
[135] Variable Energy Cyclotron Centre, Homi Bhabha National Institute, Kolkata, India

[136] Warsaw University of Technology, Warsaw, Poland
[137] Wayne State University, Detroit, Michigan, United States
[138] Yale University, New Haven, Connecticut, United States
[139] Yonsei University, Seoul, Republic of Korea
[140] Affiliated with an institute covered by a cooperation agreement with CERN
[141] Affiliated with an international laboratory covered by a cooperation agreement with CERN.